J|A|C|S
ARTICLES

Published on Web 01/07/2010

The Two Enantiomers of Citalopram Bind to the Human Serotonin Transporter in Reversed Orientations

Heidi Koldsø,[‡] Kasper Severinsen,[§] Thuy Tien Tran,[‡] Leyla Celik,[†,‡] Henrik Helligsø Jensen,[‡] Ove Wiborg,[*,§] Birgit Schiøtt,[*,†,‡] and Steffen Sinning[§]

Center for Insoluble Protein Structures (inSPIN), Interdisciplinary Nanoscience Center (iNANO), and Department of Chemistry, Aarhus University, Langelandsgade 140, DK-8000 Aarhus C, Denmark, and Laboratory of Molecular Neurobiology, Centre for Psychiatric Research, Aarhus University Hospital, Risskov, Denmark

Received August 17, 2009; E-mail: birgit@chem.au.dk; owiborg@post.tele.dk

Abstract: The two enantiomers of the antidepressant citalopram inhibit the human serotonin transporter substantially differently. Previous studies revealed Tyr95 and Ile172 as important for citalopram binding, however, the overall orientation of the ligands in the binding site and the protein−ligand interaction points remain unknown. The binding of *S*- and *R*-citalopram to a human serotonin transporter homology model are herein examined *via* docking simulations including induced fit effects. For a better description of the formal charges of the ligand when bound inside the protein, polarization effects of the protein were included by additional quantum-polarized ligand docking calculations, where ligand charges are evaluated using QM/MM calculations. By this approach a much clearer picture emerged of the positions of the functional groups of citalopram. The two enantiomers are predicted to bind in the substrate binding pocket with opposite orientations of their aromatic groups. The predicted binding modes are experimentally validated using human wild type and 15 serotonin transporter mutants and 13 optically pure citalopram analogues. Important protein−ligand interaction points were identified validating one binding model for each enantiomer. In the validated model of the high affinity enantiomer, *S*-citalopram, the fluorine atom is located near Ala173 and Thr439 and the cyano group is in close proximity of Phe341; these contacts are found to be reversed for the *R*-enantiomer.

Introduction

Depression, according to the World Health Organization, is projected to be the second largest global health problem by 2020.[1] Already, depression is the leading cause of disability measured as years lived with disease. Pharmacological treatment of depression still suffers from (i) latency periods of 3−4 weeks, (ii) a high percentage of nonresponding patients, and (iii) an ensemble of side effects,[2] all warranting research into the design of novel antidepressant medicine. Rational design of more effective drugs, however, is currently impeded by the minimal understanding of the molecular basis of affinity and selectivity.

Chemical signaling by monoamines in the central nervous system (CNS) is dependent on extracellular neurotransmitter levels which are modulated by clearance and uptake into neurons and glial cells by the human serotonin (hSERT), norepinephrine (hNET), and dopamine (hDAT) transporters, which are collectively known as the monoamine transporters (MATs). By active depletion of biogenic amines from extracellular spaces, the MATs modulate e.g. appetite, sleep, reward, sexual drive, fear, and motivation.[3]

Most clinically effective antidepressants exercise their effect by selectively inhibiting a distinct MAT or a combination of MATs.[4] The widely used antidepressant citalopram, **1**, is the most selective of the selective serotonin reuptake inhibitors (SSRIs).[5] Citalopram possesses one chiral center leading to two enantiomeric forms; *S*- and *R*-citalopram. In the 1990s, it was found that the high affinity and selectivity of citalopram for hSERT to a large degree resides in the *S*-enantiomer,[6] which in addition was found to be capable of self-potentiating its effect through a stabilizing allosteric mechanism, a property not seen for the *R*-enantiomer.[7,8] However, *R*-citalopram has been shown to be capable of allosterically effecting the dissociation of other hSERT inhibitors.[9] The favorable properties of *S*-citalopram led

[†] Center for Insoluble Protein Structures (inSPIN), Interdisciplinary Nanoscience Center (iNANO), Aarhus University.
[‡] Department of Chemistry, Aarhus University.
[§] Laboratory of Molecular Neurobiology, Centre for Psychiatric Research, Aarhus University Hospital.

(1) http://www.who.int/mental_health/management/depression/definition/en/index.html, 2009.
(2) Stahl, S. M. *Essential Psychopharmacology: the Prescriber's Guide: Antipsychotics and Mood Stabilizers*; Cambridge University Press, New York, 2006.
(3) Gether, U.; Andersen, P. H.; Larsson, O. M.; Schousboe, A. *Trends Pharmacol. Sci.* **2006**, *27*, 375–383.
(4) Andersen, J.; Kristensen, A. S.; Bang-Andersen, B.; Strømgaard, K. *Chem. Commun.* **2009**, 3677–3692.
(5) Hyttel, J. *Int. Clin. Psychopharmacol.* **1994**, *9*, 19.
(6) Hyttel, J.; Bøgesø, K. P.; Perregaard, J.; Sánchez, C. *J. Neural Transm.* **1992**, *88*, 157–160.
(7) Chen, F.; Larsen, M. B.; Sánchez, C.; Wiborg, O. *Eur. Neuropsychopharmacol.* **2005**, *15*, 193–198.
(8) Chen, F.; Larsen, M. B.; Neubauer, H. A.; Sánchez, C.; Plenge, P.; Wiborg, O. *J. Neurochem.* **2005**, *92*, 21–28.
(9) Plenge, P.; Gether, U.; Rasmussen, S. G. *Eur. J. Pharmacol.* **2007**, *567*, 1–9.

to the launch of the pure *S*-enantiomer as a new antidepressant with a faster onset of action.[10]

No crystal structures of the MATs are available. However, the emergence of a high-resolution crystal structure of a hSERT homologous protein, the leucine transporter from *Aquifex aeolicus* (LeuT),[11] made it possible to create homology models of the MATs based on the LeuT template.[12−16] The LeuT structure has also been crystallized with different antidepressants bound in a diffuse versatile site in the extracellular vestibule, termed the S2-site, leading to the central substrate site.[17−19] However, the bacterial transporter binds the antidepressants with very low affinity in a noncompetitive manner,[20] whereas the high-affinity binding of antidepressants to the homologous mammalian neurotransmitter transporters is competitive,[21−25] indicative of a binding site overlapping the substrate.[16,26,27] Furthermore, the ion dependence of an antidepressant mirrors the substrate,[28−33] and it remains inconclusive which relevance, if any, the vestibular binding site of LeuT has for hSERT inhibitor binding.[20]

Experimental attempts to describe how the two enantiomers bind to hSERT have appeared, and structural determinants for citalopram binding have been identified.[34−36] Two molecular docking studies of *S*-citalopram have recently emerged considering only one possible binding orientation of *S*-citalopram in the central binding cavity.[12,16] To the best of our knowledge the different binding patterns of *S*- and *R*-citalopram to hSERT have not previously been addressed.

In this contribution, we report the results from docking calculations of *S*- and *R*-citalopram in a refined homology model of hSERT, evaluating several ligand orientations. The possible orientations of the bound ligands were experimentally examined according to the Paired Mutant Ligand Analog Complementation (PaMLAC) paradigm.[15] By determining uptake inhibition potency of optically pure citalopram analogues for 15 single-point mutants and wild-type (wt) hSERT we identify specific protein−ligand interaction points validating the predicted binding modes. This method has previously been applied by us to characterize the binding mode of serotonin (5-HT)[15] and the tricyclic antidepressant (TCA) imipramine[27] (Chart 1) in the central binding site of hSERT. In this study 13 optically pure *S*- and *R*-citalopram, *S*-**1**, *R*-**1**, and analogues were employed (Chart 1) to avoid ambiguous data arising from binding of a racemic sample[7] and to allow detection of possible disparate orientations of the two enantiomers.

Consequently, we have resolved the protein−ligand interactions proposed for each of the enantiomers and have traced the differences between the binding modes of *S*- and *R*-citalopram. We find that citalopram binds to the central binding site overlapping with the substrate site. Additionally, we find that the positions of the two aromatic substituents, F and CN, are inverted between the two enantiomers.

Experimental Methods

Organic Synthesis. *S*-citalopram (*S*-**1**), *S*-demethylcitalopram (*S*-**2**), *S*-didemethylcitalopram (*S*-**3**), and antipodes thereof (*R*-**1**, *R*-**2**) were generous gifts from H. Lundbeck A/S. Ethyl esters (*S*-**6**, *R*-**6)** and hydroxymethyl analogues (*S*-**7**, *R*-**7**) were synthesized from *S*-**1** and *R*-**1** as described in the Supporting Information.

Citalopram analogues with a hydroxylmethyl replacing the fluorine atom (*S*-**4**, *R*-**4**) and without the cyano substituent (*S*-**5**, *R*-**5**) were synthesized as racemates using the double Grignard approach and later separated by chiral supercritical fluid chromatography (SFC); for synthetic details and establishment of absolute configurations, see the Supporting Information.

Site-Specific Mutagenesis. Mutations were introduced by PCR using the Phusion High-Fidelity DNA polymerase (Finnzymes) and primers with appropriate nucleotide mismatches followed by DpnI digestion of the parent DNA. *Escherichia coli* XL10 (Stratagene) were transformed with the mutated DNA and used for DNA production. Mutant constructs were sequenced across the entire reading frame to ensure that no unwanted mutations had been introduced.

Cell Culture and Expression of hSERT Constructs. The human embryonic kidney cell line HEK-293-MSR was grown and transfected as previously described.[15]

5-HT Uptake Assays. 5-HT uptake kinetics and IC_{50} determinations were measured 40−50 h after transfection as previously described.[15] K_i's are the mean from at least three independent experiments.

Data Calculations. IC_{50} data were fitted to sigmoidal dose−response curves with variable slope by nonlinear regression analysis in Prism 3.0 (Graphpad). K_i values were calculated from IC_{50} values

(10) Moore, N.; Verdoux, H.; Fantino, B. *Int. Clin. Psychopharmacol.* **2005**, *20*, 131–137.
(11) Yamashita, A.; Singh, S. K.; Kawate, T.; Jin, Y.; Gouaux, E. *Nature* **2005**, *437*, 215–223.
(12) Jørgensen, A. M.; Tagmose, L.; Jørgensen, A. M. M.; Topiol, S.; Sabio, M.; Gundertofte, K.; Bøgesø, K. P.; Peters, G. H. *ChemMedChem* **2007**, *2*, 815–826.
(13) Beuming, T.; Kniazeff, J.; Bergmann, M. L.; Shi, L.; Gracia, L.; Raniszewska, K.; Newman, A. H.; Javitch, J. A.; Weinstein, H.; Gether, U.; Loland, C. J. *Nat. Neurosci.* **2008**, *11*, 780–789.
(14) Indarte, M.; Madura, J.; Surratt, C. *Proteins Struct., Funct., Bioinf.* **2008**, *70*, 1033–1046.
(15) Celik, L.; Sinning, S.; Severinsen, K.; Hansen, C.; Møller, M.; Bols, M.; Wiborg, O.; Schiøtt, B. *J. Am. Chem. Soc.* **2008**, *130*, 3853–3865.
(16) Andersen, J.; Taboureau, O.; Hansen, K. B.; Olsen, L.; Egebjerg, J.; Strømgaard, K.; Kristensen, A. S. *J. Biol. Chem.* **2009**, *284*, 10276–10284.
(17) Zhou, Z.; Zhen, J.; Karpowich, N. K.; Goetz, R. M.; Law, C. J.; Reith, M. E. A.; Wang, D.-N. *Science* **2007**, *317*, 1390–1393.
(18) Zhou, Z.; Zhen, J.; Karpowich, N. K.; Law, C. J.; Reith, M. E. A.; Wang, D. *Nat. Struct. Mol. Biol.* **2009**, *16*, 652–658.
(19) Singh, S. K.; Yamashita, A.; Gouaux, E. *Nature* **2007**, *448*, 952–956.
(20) Rudnick, G. *ACS Chem. Biol.* **2007**, *2*, 606–609.
(21) Apparsundaram, S.; Stockdale, D. J.; Henningsen, R. A.; Milla, M. E.; Martin, R. S. *J. Pharmacol. Exp. Ther.* **2008**, *327*, 982–990.
(22) Hyttel, J. *Psychopharmacology* **1977**, *51*, 225–233.
(23) Talvenheimo, J.; Nelson, P. J.; Rudnick, G. *J. Biol. Chem.* **1979**, *254*, 4631.
(24) Thomas, D. R.; Nelson, D. R.; Johnson, A. M. *Psychopharmacology* **1987**, *93*, 193–200.
(25) Humphreys, C. J.; Levin, J.; Rudnick, G. *Mol. Pharmacol.* **1988**, *33*, 657–663.
(26) Graham, D.; Esnaud, H.; Langer, S. Z. *Biochem. Pharmacol.* **1989**, *38*, 3819–3826.
(27) Sinning, S.; Musgaard, M.; Jensen, M.; Severinsen, K.; Celik, L.; Koldsø, H.; Meyer, T.; Bols, M.; Jensen, H. H.; Schiøtt, B.; Wiborg, O. *J. Biol. Chem.* [Online early access]. DOI: 10.1074/jbc.M109.045401. Published Online: Nov 30, 2009.
(28) Lee, C. M.; Javitch, J. A.; Snyder, S. H. *J. Neurosci.* **1982**, *2*, 1512–1525.
(29) Lee, C. M.; Snyder, S. H. *Proc. Natl. Acad. Sci. U.S.A.* **1981**, *78*, 5250–5254.
(30) Lingjaerde, O. J. *Acta Physiol. Scand.* **1971**, *81*, 75–83.
(31) Humphreys, C. J.; Wall, S. C.; Rudnick, G. *Biochemistry* **1994**, *33*, 9118–9125.
(32) Mann, C. D.; Hrdina, P. D. *J. Neurochem.* **1992**, *59*, 1856–1861.
(33) Zeitner, C. J.; Graefe, K. H. *Naunyn-Schmiedeberg's Arch. Pharmacol.* **1986**, *334*, 397–402.
(34) Barker, E. L.; Perlman, M. A.; Adkins, E. M.; Houlihan, W. J.; Pristupa, Z. B.; Niznik, H. B.; Blakely, R. D. *J. Biol. Chem.* **1998**, *273*, 19459–19468.
(35) Larsen, M. B.; Elfving, B.; Wiborg, O. *J. Biol. Chem.* **2004**, *279*, 42147–42156.
(36) Henry, L. K.; Field, J. R.; Adkins, E. M.; Parnas, M. L.; Vaughan, R. A.; Zou, M. F.; Newman, A. H.; Blakely, R. D. *J. Biol. Chem.* **2006**, *281*, 2012–2023.

Chart 1. Chemical Structures of Ligands Employed; (A) *S*- and *R*-citalopram (**1**) and Optically Pure Analogues Included in This Study; (B) Chemical Structures of Serotonin and Imipramine; for Easy Recognition, the Analogues are Named As Depicted in A; the Aromatically Substituted Analogues Use a Simple Name Scheme Where the Two Groups in the Parentheses Refer to the Substituent at the Phenyl Ring and the Substituent on the 1,3-Dihydroisobenzofuran Ring, Respectively

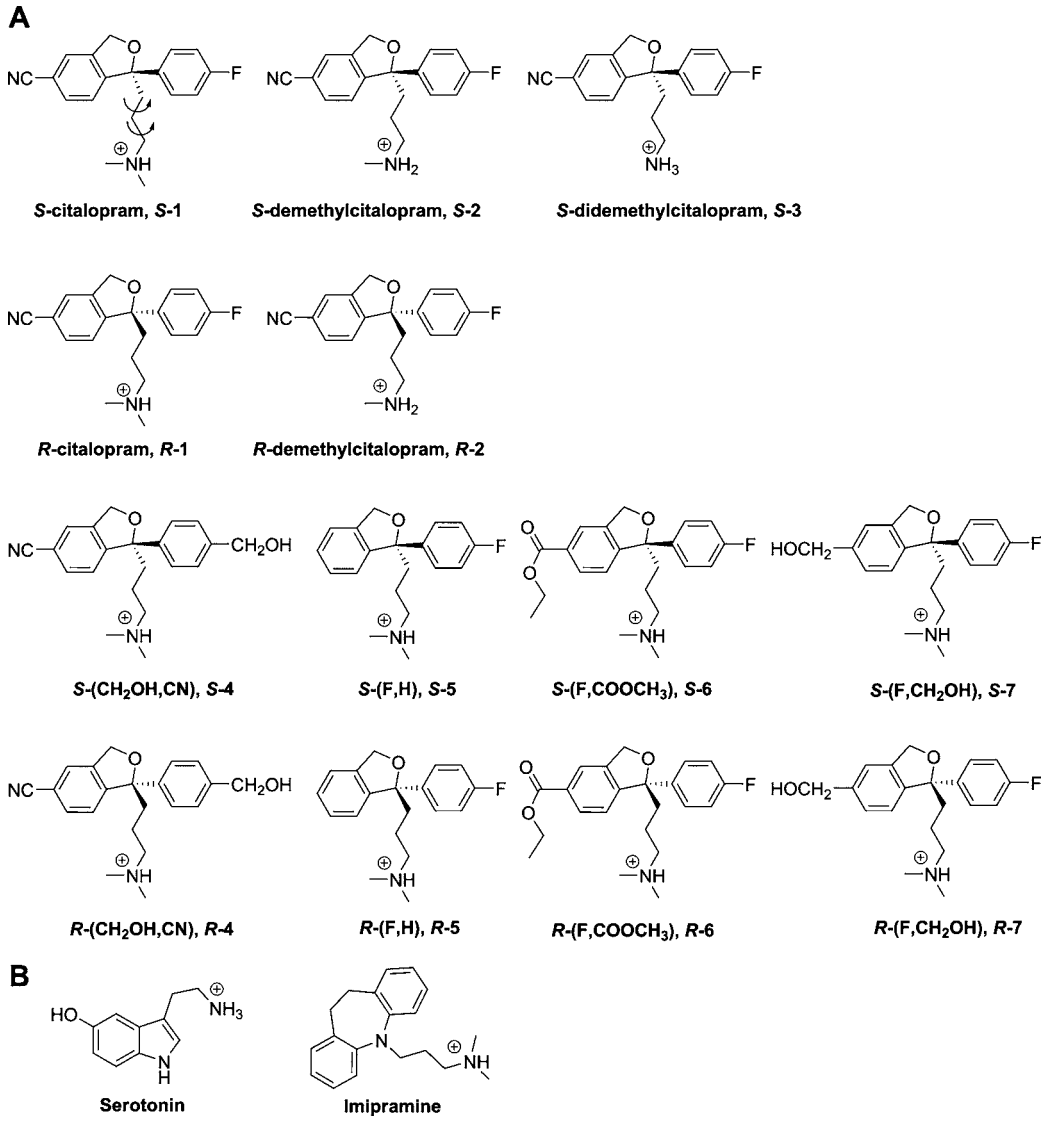

using the Cheng and Prusoff equation[37] to adjust for substrate concentration and apparent substrate affinity, K_M. Assuming Michaelis−Menten-like kinetics, K_m and V_{max} were calculated by fitting data to a one-site binding hyperbola by nonlinear regression analysis in Prism 3.0.

Computational Methods

One homology model of hSERT has been used in this study for advanced docking simulations of *S*- and *R*-citalopram including induced fit and effects of polarization by the protein on the ligand. The docking simulations were supplemented by calculations of molecular interaction fields (MIFs) and by computations of strain energies of the predicted binding modes compared to that of free citalopram. The details of all the modeling stages are provided in the Supporting Information. Below, an overview is given.

Protein Modeling. The homology model[15] was extensively refined, mostly with respect to structural elements some distance away from the substrate binding site. The two sodium ions identified in the LeuT crystal structure were included in the refined homology model with the same coordinates as in the pdb-structure (pdb-code: 2A65[11]). The chloride ion was similarly placed in the proposed binding site.[38,39] Ultimately, the hSERT C-terminus was removed. The resulting extensively refined homology model contains a total of 536 residues ranging from Arg79 to Pro614. This refined protein structure served as the input structure for the induced fit docking calculations. Please see the Supporting Information for all details of homology modeling.

Ligand Modeling. The ligands, *S*- and *R*-citalopram (*S*-**1**, *R*-**1**), were manually built and optimized as described in the Supporting Information. The tertiary amine was modeled as charged. A Monte Carlo conformational search was made to identify all low-energy conformations. The conformation with the lowest energy that did not include an intramolecular hydrogen bond was chosen as the input structure for the induced fit docking simulation.

(37) Yung-Chi, C.; Prusoff, W. H. *Biochem. Pharmacol.* **1973**, *22*, 3099–3108.

(38) Forrest, L. R.; Tavoulari, S.; Zhang, Y. W.; Rudnick, G.; Honig, B. *Proc. Natl. Acad. Sci. U.S.A.* **2007**, *104*, 12761–12766.

(39) Zomot, E.; Bendahan, A.; Quick, M.; Zhao, Y.; Javitch, J.; Kanner, B. *Nature* **2007**, *449*, 726–730.

Induced Fit Docking (IFD). The two enantiomeric forms of citalopram were docked into the refined homology model of hSERT by means of the IFD method.[40] IFD includes protein side-chain flexibility in a radius of 5.0 Å around the poses found during the initial soft docking stage of the IFD protocol.[40] The binding site for the initial docking was defined by five residues surrounding the substrate binding cavity; Asp98, Ile172, Phe341, Thr439, and Gly442; all were chosen on the basis of biochemical results and previous binding models for 5-HT[15] and imipramine in hSERT.[27] The residues chosen all line the central binding site,[15] and some have been shown to be involved in interactions with bound ligands.[35,36,41−43] Up to 100 poses were saved from each calculation, with an energy-window of 50 kcal/mol to allow for larger diversity among the output structures. The Standard Precision (SP)[44] scoring function was applied in the initial soft docking stage and the Extra Precision (XP) Glide score[45] in the redocking stage. Both of the Glide Scoring functions[44,45] are parametrized to be able to estimate binding affinities; however, it is well-known that scoring functions in docking calculations are not perfect.[46,47] Therefore, we did not rely on the top-scoring pose; rather, we saved a diverse set of poses that were further analyzed computationally and assessed experimentally. The returned poses were visually clustered by position of the three functional groups (-F, -CN, and the tertiary ammonium group) and the furan oxygen atom; the calculated RMSDs are listed in the Supporting Information.

Quantum-Polarized Ligand Docking (QPLD). A selected binding pose from each cluster for each enantiomer generated from IFD were further evaluated by QPLD.[48] QPLD is a QM/MM approach which treats the ligand with QM methods and the protein with MM. As a result, QPLD incorporates a more precise treatment of the partial charges of the ligand, which is essential for discriminating between the proposed locations of the fluorine atom and the cyano group, which are found to be the most pronounced differences between the binding models of citalopram enantiomers in hSERT. In the initial step, the QPLD protocol includes a Glide docking[44] to produce unique ligand−protein complexes. QSite[49] is then used to calculate partial atomic charges for the ligand at the B3LYP/6-31G* level of theory while inside the protein. The protein is modeled with MM methods at this stage using the OPLS-AA force field.[50] Finally, the ligand is redocked using the optimized partial charges and either the SP- or XP-scoring function in Glide.[44,45] Both of the empirical Glide scoring functions depend on the partial charges by inclusion of a scaled Coulombic term accounting for electrostatic interactions between partially charged atoms in the protein and ligand, respectively.[44,45] In the end, the energetically most favorable poses are returned. Up to 20 poses were saved from each QPLD calculation. The ligand is treated as flexible in the two docking stages, while the protein is held fixed in the conformation observed from the preceding IFD calculations.

Grid Calculations. The binding sites of the different binding modes were characterized by MIFs, which were calculated by the GRID software.[51] The probes applied were a methyl group, the sp^3-hybridized amine-NH cation, an sp-hybridized nitrogen atom with a lone-pair, a furan oxygen atom, and an organic fluorine atom.

Docking in Extracellular Vestibular S2-Site. For comparison, a series of IFD docking calculations were set up to assess the possibility of citalopram to bind in the vestibular S2-site,[17−19] which has been found for other antidepressants, not including citalopram, binding to LeuT. The S2-site was defined from residues Gly100, Tyr176, Phe335, Ile179, and Glu493.[18] *R*-Citalopram and *S*-citalopram were docked into S2 using the XP-scoring function in the redocking stage. The central substrate binding pocket was either occupied by 5-HT or citalopram, and the protein always included the ions. The results are listed in the Supporting Information.

Results

The PaMLAC strategy in this study was to initially predict likely binding models for *S*- and *R*-citalopram in hSERT by a wide palette of molecular modeling techniques. The next stage was to test the predictions made by extensive SAR-studies from uptake inhibition experiments of optically pure citalopram analogues in wt hSERT and selected mutants. The acquired data finally allowed us to decide which of the possible binding models seem most likely for each enantiomer of citalopram.

Molecular Modeling - Overview. An extensively refined homology model of hSERT has been used for docking simulations of *S*- and *R*-citalopram including protein-induced fit and polarization effects of the ligand, resulting in two possible binding modes for each enantiomer. To further assess the predicted binding modes from the docking simulation, the analyses were supplemented by calculations of MIFs and by computations of strain energies of the predicted binding modes compared to free citalopram. All modeling studies contain approximations; however, care was taken at all steps to avoid bias by using multiple methods and preventing manual manipulations.

Protein Modeling. The homology model of hSERT was refined compared to our initial homology model[15] by including additional experimental data of EL2 (see Supporting Information for details). In brief, 20 homology models were generated, and the best model was chosen on the basis of several characteristics including the probability density function (as low as possible), Ramachandran plots, size of the binding pocket (as large as possible), and rotamer conformation of Asp98. As a first test of the refined protein structure, the binding mode of the natural substrate 5-HT was compared to the previously published model.[15] The output from IFD[40] simulation of 5-HT resulted in 71 poses, of which 26 reproduced the validated binding mode,[15] thereby suggesting that the refined homology model of hSERT is at least comparable and possibly superior to the previous one.

Binding of Citalopram. The central binding cavity in the homology models of hSERT is too small to directly accommodate citalopram in a standard rigid-protein docking procedure,[12,13,15,16,27] and therefore we used IFD[40] to introduce *S*- and *R*-citalopram in the central binding site of hSERT. This resulted in a position overlapping with the one observed for the cognate substrate, 5-HT.[15] The results are shown in Table

(40) Sherman, W.; Day, T.; Jacobson, M. P.; Friesner, R. A.; Farid, R. *J. Med. Chem.* **2006**, *49*, 534–553.
(41) Barker, E. L.; Moore, K. R.; Rakhshan, F.; Blakely, R. D. *J. Neurosci.* **1999**, *19*, 4705–4717.
(42) Chen, J.; Sachpatzidis, A.; Rudnick, G. *J. Biol. Chem.* **1997**, *272*, 28321–28327.
(43) Mortensen, O. V.; Kristensen, A. S.; Wiborg, O. *J. Neurochem.* **2001**, *79*, 237–247.
(44) Friesner, R. A.; Banks, J. L.; Murphy, R. B.; Halgren, T. A.; Klicic, J. J.; Mainz, D. T.; Repasky, M. P.; Knoll, E. H.; Shelley, M.; Perry, J. K.; Shaw, D. E.; Francis, P.; Shenkin, P. S. *J. Med. Chem.* **2004**, *47*, 1739–1749.
(45) Friesner, R. A.; Murphy, R. B.; Repasky, M. P.; Frye, L. L.; Greenwood, J. R.; Halgren, T. A.; Sanschagrin, P. C.; Mainz, D. T. *J. Med. Chem.* **2006**, *49*, 6177–6196.
(46) Cheng, T.; Li, X.; Li, Y.; Liu, Z.; Wang, R. *J. Chem. Inf. Mol.* **2009**, *49*, 1079–1093.
(47) Sousa, S. F.; Fernandes, P. A.; Ramos, M. J. *Proteins* **2006**, *65*, 15–26.
(48) Cho, A. E.; Guallar, V.; Berne, B. J.; Friesner, R. *J. Comput. Chem.* **2005**, *26*, 915–931.
(49) Murphy, R. B.; Philipp, D. M.; Friesner, R. A. *J. Comput. Chem.* **2000**, *21*, 1442–1457.
(50) Kaminski, G. A.; Friesner, R. A.; Tirado-Rives, J.; Jorgensen, W. L. *J. Phys. Chem. B* **2001**, *105*, 6474–6487.
(51) Cruciani, G. *Molecular Interaction Fields: Application in Drug Design and ADME Prediction*; Mannhold, R., Kuninyi, H., Folkers, G., Eds.; Wiley-VCH: Weinheim, 2006; Vol. 27.

Table 1. Statistics for the Four Clusters Identified from the Different Docking Simulations; Mean Value Is Listed for the Distance, GlideScore, and Emodel; Standard Deviations Are Shown in Brackets

cluster/method	scoring function initial docking/ redocking	number of poses/ total poses	distance Asp98(Oδ)−N^+ (Å)	Glidescore (kcal/mol)	Emodel (kcal/mol)
S-ClusterI					
IFD	SP/XP	5/10	4.72 [0.45]	−8.6 [0.9]	−39.9 [22.4]
QPLD[a]	SP/SP	4/20	5.52 [0.04]	−8.8 [0.2]	−77.5 [0.7]
QPLD[a]	SP/XP	11/11	5.39 [0.35]	−6.7 [1.9]	−63.9 [5.3]
QPLD[a]	XP/XP	4/4	5.56 [0.52]	−5.9 [3.1]	−65.8 [3.3]
total of all *S* Poses		24/91	5.30 [0.48]	−7.0 [2.1][b]	−61.5 [15.4]
S-ClusterII					
IFD	SP/XP	2/10	3.97 [0.56]	−10.5 [0.6]	−66.0 [24.0]
QPLD[a]	SP/SP	20/20	4.46 [0.07]	−10.4 [0.2]	−98.1 [5.3]
QPLD[a]	SP/XP	18/18	4.24 [0.25]	−10.8 [0.3]	−86.4 [1.4]
QPLD[a]	XP/XP	8/8	4.13 [0.17]	−10.9 [0.2]	−86.5 [1.6]
total of all *S* Poses		64/91	4.30 [0.24]	−10.8 [0.3][b]	−90.4 [9.2]
R-ClusterI					
IFD	SP/XP	3/6	3.83 [0.58]	−8.4 [0.2]	−34.1 [2.7]
QPLD[a]	SP/SP	15/20	3.25 [0.11]	−8.0 [0.2]	−54.7 [6.5]
QPLD[a]	SP/XP	8/9	3.19 [0.15]	−8.3 [0.5]	−37.2 [2.2]
QPLD[a]	XP/XP	3/3	3.24 [0.19]	−8.8 [0.1]	−42.0 [1.5]
total of all *R* Poses		40/74	3.29 [0.27]	−8.4 [0.4][b]	−47.1 [10.0]
R-ClusterII					
IFD	SP/XP	2/6	4.52 [0.13]	−10.1 [0.1]	−13.7 [0.3]
QPLD[a]	SP/SP	12/20	4.67 [0.05]	−8.4 [0.3]	−37.7 [2.2]
QPLD[a]	SP/XP	10/13	4.67 [0.10]	−7.8 [2.2]	−21.7 [2.9]
QPLD[a]	XP/XP	3/3	4.50 [0.14]	−8.1 [1.9]	−19.4 [3.2]
total of all *R* Poses		33/74	4.61 [0.10]	−8.1 [2.2][b]	−28.2 [9.2]

[a] For some of the QPLD-setups, the ligand changes cluster upon docking; these poses are only included in the total statistics for the number of poses and not in the calculated average properties. [b] These values are only from the docking using the XP scoring function.

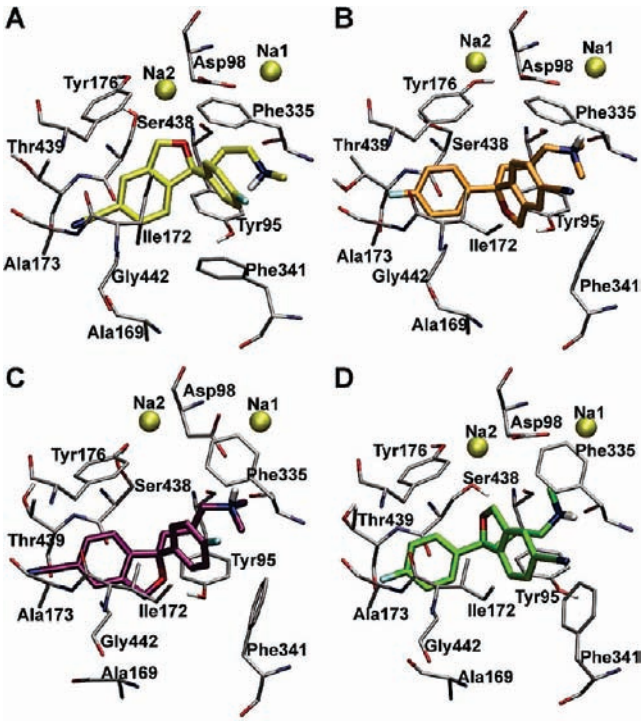

Figure 1. The four identified binding clusters for *S*- and *R*-citalopram; the two clusters of *S*-citalopram are seen in (A) ***S*-ClusterI** (yellow) and (B) ***S*-ClusterII** (orange). The two clusters of *R*-citalopram are (C) ***R*-ClusterI** (purple) and (D) ***R*-ClusterII** (green). hSERT is shown in the same overall orientation in all panels.

1. Two clusters (***S*-ClusterI** and ***S*-ClusterII**) were identified from IFD of *S*-**1** (Figure 1 A and B) with primary differences being the orientation of the fluoro and cyano substituents. IFD of *R*-**1** also yielded two clusters, ***R*-ClusterI** and ***R*-ClusterII** (Figure 1 C and D). In all clusters identified, the ion binding sites were unaffected by the induced fit of the protein during the IFD protocol. The orientation of *R*-citalopram in these two clusters was also internally reversed with respect to the fluoro and cyano substituents resulting in a similar overall occupation of the binding site by citalopram in the four clusters, see Figure 1. In two of the identified clusters, ***S*-ClusterII** and ***R*-ClusterI**, the positively charged tertiary ammonium group can form an ion-pair interaction[52] with the acidic side chain of Asp98 (Table 1), similarly to the results for 5-HT,[15,53] TCAs, and other antidepressants.[16,27] Furthermore, the dihedral angles of the propyl amine group are found in either the (*gauche*,*gauche*), (*anti*,*anti*), or (*anti*,*gauche*) conformations (Supporting Information, Tables S1 and S2).

Residues lining the pocket harboring the *N*,*N*-dimethylaminopropyl side chain are Tyr95, Ala96, Asp98, Phe334, Phe335, Ser336, Leu337, Gly338, and Phe341. In ***S*-ClusterI** (Figure 1 A) of *S*-citalopram the fluorophenyl group is located in a binding pocket lined by Thr497, Phe335, Phe341, and Val501, whereas the cyano group is in close proximity to Ala169, Ala173, Asn177, Ser438, Thr439, and Leu443 (for clarity, not all mentioned residues are shown in the figure). Several of the residues coordinating the cyano group of *S*-**1** also line the hydrophilic pocket harboring the hydroxyl group of 5-HT.[15] The other cluster of *S*-**1**, ***S*-ClusterII** (Figure 1 B), has the two aromatic substituents oriented oppositely, relative to ***S*-ClusterI**. Consequently, in ***S*-ClusterII** the fluorophenyl group is harbored by the hydrophilic pocket lined by Ala169, Ala173, Asn177, Ser438, Thr439, and Leu443, whereas the cyano group is close to Thr497, Phe335, Phe341, and Val501. Similar observations are found for the two *R*-citalopram clusters; ***R*-ClusterI** (Figure 1 C) is found to include the same positions of the aromatic

(52) Barlow, D. J.; Thornton, J. M. *J. Mol. Biol.* **1983**, *168*, 867–885.
(53) Barker, E. L.; Blakely, R. D. *Methods Enzymol.* **1998**, *296*, 475–498.

substituents of *R*-**1** as was seen in the ***S*-ClusterI** of the *S*-enantiomer. This can be accomplished by an approximately 180° rotation of the dihydroisobenzofuran ring around the stereogenic center, which then comprises the only major difference between ***R*-ClusterI** and ***S*-ClusterI**. Similarly, the orientation of the dihydroisobenzofuran system constitutes the only significant difference between ***R*-ClusterII** and ***S*-ClusterII** (Figure 1 D). Because of the ubiquitous Asp98···dimethylammonium interaction, the differences in overall placement of the inhibitor binding poses in the central binding cavity can only be discerned by the different position of the two aromatic substituents, -F and -CN, respectively, in the two binding models for each enantiomer of citalopram.

Quantum-Polarized Ligand Docking (QPLD). A remarkable difference between the two binding modes for each enantiomer is the positions of the fluoro and the cyano substituents. To more appropriately model these two functional groups, which are the presumed anchor points in the protein−ligand complexes, QPLD simulations were carried out.[48] This method uses quantum mechanics to calculate partial atomic charges for the ligand inside the binding pocket, thereby taking protein polarization effects into account and providing a superior description of these important functional groups.[48] It has been shown that polarization of the ligand upon binding is important for reliably predicting the binding mode of small molecules with polarizable groups.[48]

The best poses from IFD were subjected to the QPLD simulations (Table 1). The results reveal that the *N*-methyl groups of citalopram are polarized much more than in the OPLS force field with the three hydrogen atoms at each methyl group having a partial charge of approximately +0.2. This polarization accounts for the observed changes with QPLD. When the number of poses in a given cluster in Table 1 after QPLD does not equal the total number of returned poses, a shift to the other cluster has taken place. It is noteworthy that for *S*-citalopram, all ***S*-ClusterII** poses stay in this cluster, contrary to ***S*-ClusterI** where QPLD, with the SP scoring function, only returns four structures out of 20 possible poses belonging to ***S*-ClusterI**. Consequently, the rest end up in ***S*-ClusterII**. The shift may indicate a preference for ***S*-ClusterII** when the polarizing effect of the surrounding protein is taken into account. This is further substantiated by the fact that QPLD for ***S*-ClusterII** yields more poses overall with no shifts to the other cluster. For *R*-citalopram, changes in cluster populations are also observed. However, this time it is found for both ***R*-ClusterI** and ***R*-ClusterII** during the QPLD calculations. The relative number of shifts is largest from ***R*-ClusterII** into ***R*-ClusterI**, which may indicate a small preference for a binding mode as in ***R*-ClusterI**.

It is evident from the computed docking scores (Table 1) that ***S*-ClusterII** obtains a significant better average GlideScore among the four clusters consistent with the fact that *S*-**1** displays a better affinity for hSERT than *R*-**1**. Again, this observation indicates that ***S*-ClusterII** is the more favorable of the two *S*-citalopram clusters. It is not possible to differentiate between the two clusters of *R*-citalopram solely from the GlideScore, but the population of poses and the stretched ionic interaction of ***R*-ClusterII** with Asp98 may indicate a slight preference for ***R*-ClusterI**.

Central Binding Site Characterization. In order to gain further knowledge about the properties of the central binding cavity of hSERT, we performed GRID-calculations[54] establishing MIFs to map the most favorable regions for placing the distinct anchor-points of citalopram, *i.e*. the ammonium center, the furan oxygen, the fluorine atom, and the cyano group (Figure 2). Since IFD introduces protein flexibility, the MIFs of a pose representing each of the four identified clusters were calculated. The MIFs resulting from probes for an organic fluorine atom and a sp-hybridized nitrogen atom with a lone-pair could not unambiguously differentiate between the clusters since all four binding modes of the ligand could fit into these MIFs, similar to what has been observed by others.[12] It can be seen that only ***S*-ClusterII** (Figure 2 C) and ***R*-ClusterI** (Figure 2 B) fits well into the defined space for the furan oxygen probe. The preferred placement of the positively charged ammonium ion overlaps for all four clusters and is close to Asp98, as shown for ***S*-ClusterII** (Figure 2 E). Two almost equally favorable areas are found between Asp98 and Tyr95, and Asp98 and Ser438, respectively. Only one of the poses generated for *S*-**1** places the ammonium ion in the latter position. The results from the hydrophobic probe (C3) also resemble each other for the different clusters (***S*-ClusterII** with C3 probe is depicted in Figure 2 F), substantiating that the hydrophobic core of the citalopram skeleton must be placed in this area.

Internal Energy of Bound Citalopram. To additionally characterize the most favorable binding mode of each enantiomer of citalopram, the conformational energy of the bound ligand was compared to the energy of the global minimum in water. The global energy minimum structure, which did not possess an intramolecular hydrogen bond, was identified from a Monte Carlo conformational search. An energy difference of 3 kcal/mol between the global energy minimum and bioactive conformations of high affinity ligands has earlier been recommended as an acceptable upper limit for steric strain introduced in a small molecule ligand upon binding to a protein.[55] In an identical manner, for each of four clusters, we determined the conformational energy difference between the bioactive conformation and the global energy minimum attained from an aqueous conformational ensemble resulting from the conformational search in continuum solvent. The energy differences between the energy minimized bioactive conformation and the global energy minimum of each of the four clusters were found to be; 3.62 kcal/mol (***S*-ClusterI**); 2.20 kcal/mol (***S*-ClusterII**); 2.14 kcal/mol (***R*-ClusterI**), and 2.57 kcal/mol (***R*-ClusterII**), with RMSDs of the heteroatoms measuring at 0.28, 0.63, 0.36, and 0.38 Å between the bioactive conformation and the corresponding conformation from the conformational ensemble, respectively. These values indicate that binding models as in ***S*-ClusterII, *R*-ClusterI,** and ***R*-ClusterII** all are in the acceptable range of the global minimum, whereas ***S*-ClusterI** is less likely. Again, this observation suggests that ***S*-ClusterII** is the most probable representation of *S*-citalopram binding in hSERT.

To summarize, the GlideScore, the ionic interaction distance between Asp98 and the ammonium ion of the ligand, the QPLD populations and scores, the GRID calculation, as well as the calculated energy difference between the global minimum and bioactive conformation, all points toward ***S*-ClusterII** as the most likely binding mode of the high affinity *S*-enantiomer of citalopram. The picture is less clear concerning the low affinity *R*-enantiomer. However, the distance of the ionic interaction to

(54) http://www.moldiscovery.com/soft_grid.php.
(55) Boström, J.; Norrby, P.-O.; Liljefors, T. *J. Comput.-Aided Mol. Des.* **1998**, *12*, 383–383.

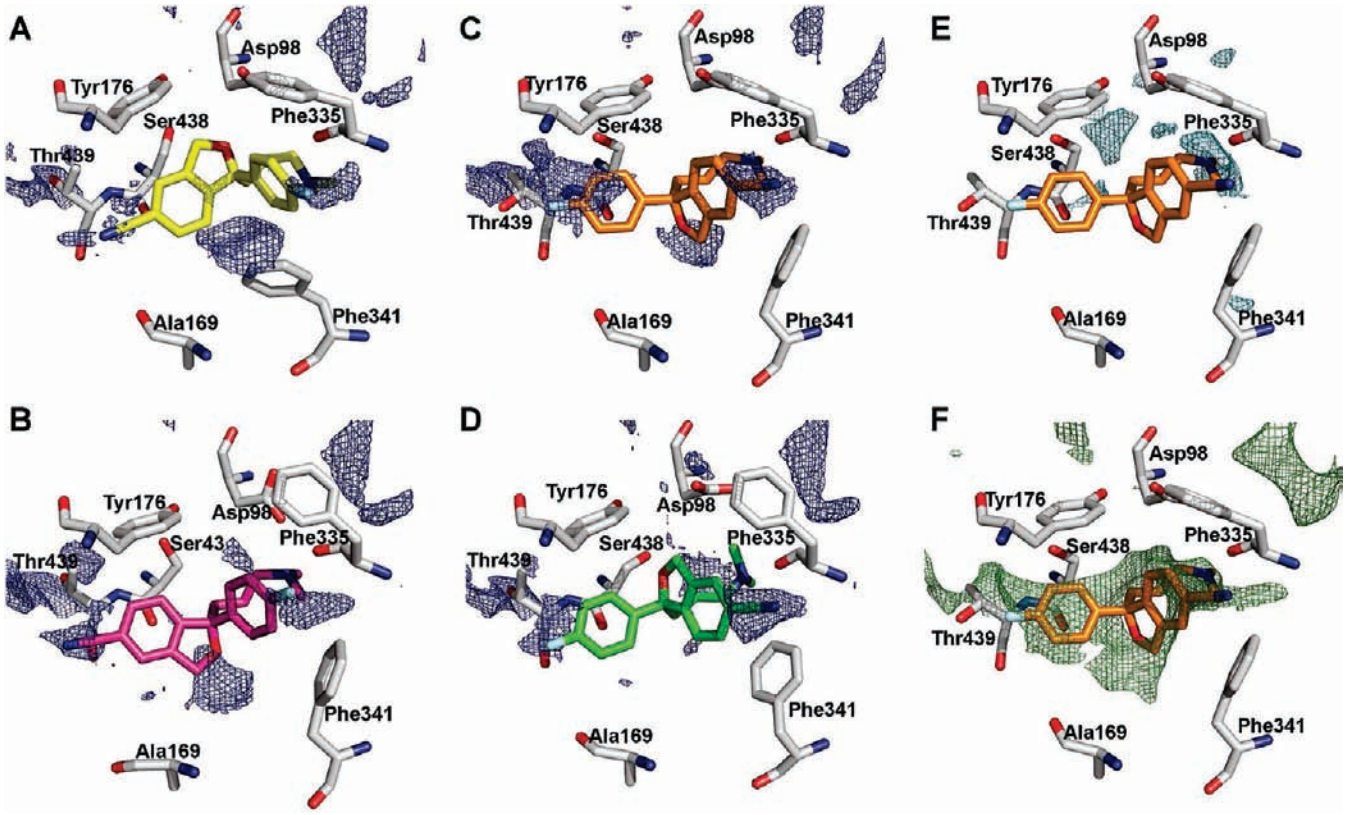

Figure 2. Examples of computed MIF-fields from the GRID calculations for *R*- and *S*-citalopram bound to hSERT. The MIFs resulting from the furan oxygen probe at an energy level −3.0 kcal/mol are shown for (A) ***S*-ClusterI**, (B) ***R*-ClusterI**, (C) ***S*-ClusterII** and (D) ***R*-ClusterII**. (E) Calculated MIF resulting from an ammonium ion-probe at an energy level −15.0 kcal/mol for ***S*-ClusterII**. (F) ***S*-ClusterII** and the MIF from the calculation with the hydrophobic C3 probe at an energy level −3.0 kcal/mol.

Table 2. Mean K_i Values (nM) and 95% Confidence Intervals (in Brackets) for Inhibition of ^{3}H-5-HT Uptake by HEK-293 MSR Cells Transiently Transfected with Different hSERT Mutants

	hSERT wt	Tyr95Phe	Asp98Glu	Ser438Thr
S-citalopram, *S*-**1**	9.2 [5.6−15.2]	132 [54−320]	560 [310−1000]	2000 [310−13000]
S-demethylcitalopram, *S*-**2**	48 [25−90]	61 [23−163]	770 [300−1950]	1620 [700−3800]
S-didemethylcitalopram, *S*-**3**	520 [190−1440]	860 [340−2200]	170 [95−300]	360 [63−2000]
R-citalopram, *R*-**1**	370 [250−540]	820 [370−1780]	1740 [1060−2800]	20000 [14900−29000]
R-demethylcitalopram, *R*-**2**	37 [21−64]	39 [34−45]	240 [71−780]	101 [15−680]

Asp98, the populations from the QPLD calculations as well as the GRID calculations indicate that ***R*-ClusterI** is most favorable.

PaMLAC Validation of Citalopram Orientation in hSERT - Overview. The PaMLAC method was used to explore the modeled orientations of *S*- and *R*-citalopram. Uptake inhibition experiments were conducted employing complementary combinations of mutated hSERT and citalopram analogues to establish the most likely position of the three distinct functional groups (the fluoro, cyano, and dimethylammonium groups of citalopram). The PaMLAC method was previously used by us to provide experimental support for the IFD models of 5-HT[15] and TCAs in hSERT.[27] The effectiveness of PaMLAC depends greatly on the availability of a sufficient repertoire of both protein mutants and complementary ligand analogues to identify direct interaction points. In the present study we identify interaction partners for the three most distal functionalities of citalopram which unambiguously orientate the ligand within the binding site. We do this by examining wt hSERT along with 15 single-point mutants for their affinity against 13 optically pure citalopram analogues (Chart 1 A). The strategy for choosing the analogues was to either remove one or both of the *N*-methyl groups or to remove or replace one of the two aromatic substituents of citalopram, -F or -CN, by another functional group. Variation of a single structural parameter on the inhibitor allowed for efficient exploration of the protein environment around the tertiary ammonium functionality as well as the fluorine and cyano substituents of the enantiomers of each analogue. Mutants included in the PaMLAC study were similarly chosen to precisely explore the predicted protein−ligand interactions from the IFD study. The single-point mutants of hSERT covered the majority of residues that interact with leucine in the LeuT structure,[11] and include both hydrophobic and hydrophilic residues at each mutated position. The result for *S*- and *R*-citalopram analogues with varying degree of *N*-methylation are listed in Table 2 and with no or different groups at the 4-position of the phenyl ring and the 5-position of the dihydroisobenzofuran ring can be seen in Table 3.

***S*-Citalopram - Ammonium Ion.** Aside from the salt-bridge to Asp98 observed in ***S*-ClusterII,** the positively charged ammonium ion in both clusters occupies the space between the negatively charged carboxylic acid of Asp98 and the electron-rich side chain of Tyr95. The tertiary ammonium center thus

Table 3. Mean K_i Values (nM) and 95% Confidence Intervals (in Brackets) for Inhibition of ^{3}H-5-HT Uptake by HEK-293 MSR Cells Transiently Transfected with Different hSERT Mutants

	S-(F,CN), *S*-**1** nM	*S*-(CH_2OH,CN), *S*-**4** nM	*S*-(F,H), *S*-**5** nM	*S*-(F,COOEt), *S*-**6** nM	*S*-(F,CH_2OH), *S*-**7** nM
wt hSERT	9.2 [5.6−15.2]	83 [61−114]	54 [48−61]	86 [45−161]	60 [45−79]
Ala173Ser	7.7 [1.73−35]	87 [42−176]	48 [19.7−116]	131 [62−280]	91 [51−163]
Ala173Met	4.1 [1.51−11]	4000 [2700−6000]	50 [6.2−410]	60 [4.8−740]	110 [60−199]
Tyr175Phe	3.6 [1.25−10.1]	37 [14.5−96]	26 [6.3−105]	23 [12.3−43]	12.5 [1.29−121]
Tyr176Phe	15.4 [10.6−22]	230 [81−680]	145 [49−430]	280 [128−600]	156 [53−460]
Phe335Asn	9.6 [5.4−17.3]	135 [67−270]	68 [47−97]	177 [90−350]	34 [12.1−94]
Phe335Tyr	4.9 [0.56−43]	28 [0.7−1120]	19.1 [4−90]	48[a]	23 [13.1−42]
Phe341Tyr	1520 [1370−1680]	19400 [4300−87000]	1910 [1560−2300]	2400[a]	960 [650−1420]
Thr439Ala	4.2 [1.51−11.5]	59 [28−120]	54 [38−76]	49 [22−109]	24 [5.1−114]
Thr439Ser	8.8 [4.6−16.7]	31 [23−42]	82 [39−172]	102 [45−230]	76 [37−157]
Asn177Ala	78 [42−144]	10100 [8500−12000]	530 [240−1150]	390 [152−980]	340 [94−1260]
Asn177Ser	220 [154−320]	10600 [5000−23000]	1110 [700−1760]	530 [270−1030]	1402 [610−3200]
Asn177Thr	111 [76−163]	9300 [6000−14500]	720 [430−1200]	350 [210−570]	623 [450−870]

	R-(F,CN), *R*-**1** nM	*R*-(CH_2OH,CN), *R*-**4** nM	*R*-(F,H), *R*-**5** nM	*R*-(F,COOEt), *R*-**6** nM	*R*-(F,CH_2OH), *R*-**7** nM
hSERT wt	370 [250−540]	1050 [680−1620]	730 [460−1150]	1930 [1000−3900]	590 [460−760]
Ala173Ser	220 [82−600]	740 [82−6600]	152 [57−400]	1020 [440−2400]	370 [154−880]
Ala173Met	149 [52−430]	680 [590−790]	73 [30−175]	750 [250−2200]	540 [300−960]
Tyr175Phe	84 [28−250]	390 [105−1470]	162 [15.7−1680]	380 [66−2200	67 [19.5−230]
Tyr176Phe	1560 [700−3500]	3200 [680−14600]	2000 [950−4400]	5500 [2700−11200]	1700 [540−5300]
Phe335Asn	340 [183−640]	2100 [850−5000]	660 [360−1210]	1000 [166−6000]	460 [188−1140]
Phe335Tyr	86 [24−300]	390 [67−2200]	250 [89−690]	630[a]	133 [1.43−12400]
Phe341Tyr	2200 [1620−2900]	5800 [1350−25000]	4900 [2600−8900]	6600[a]	2800 [1370−5700]
Thr439Ala	240 [151−380]	910 [460−1810]	250 [109−570]	560 [200−1500]	210 [64−680]
Thr439Ser	176 [116−270]	680 [240−1910]	280 [175−430]	2100 [1000−4500]	106 [49−228]
Asn177Ala	6600 [4500−9600]	54000 [41000−70000]	3000 [2300−3700]	5600 [4400−7200]	6400 [6200−6600]
Asn177Ser	7300 [3500−15000]	66000 [2000−221000]	7100 [4200−12300]	5200 [3700−7200]	12300 [4400−34000]
Asn177Thr	5300 [3000−9400]	44000 [36000−54000]	3000 [2100−4300]	4500 [2500−7800]	6900 [3600−13400]

[a] Experiment repeated once.

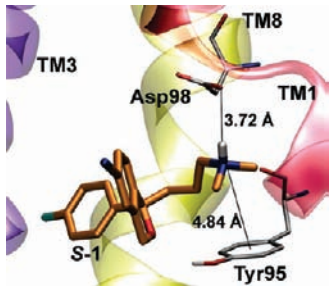

Figure 3. Binding of *S*-citalopram in hSERT. The positive charge of the ammonium ion can be stabilized by bridging the carboxylate group of Asp98 and the π-electrons of Tyr95 through an aromatic amine[56] interaction.

can participate in an amino-aromatic interaction[56] with Tyr95 and furthermore in a stabilizing interaction between one of the *N*-methyls by the hydroxyl group of Tyr95 (Figure 3). The charged nitrogen atom is favorably placed about 4.8 Å above the centroid of the aromatic ring.

The interaction between the ammonium ion of the ligand and the electron-rich pocket of the protein was examined by measuring the inhibitory potencies of *S*-citalopram (*S*-**1**) and its less methylated analogues, *S*-demethylcitalopram (*S*-**2**) and *S*-didemethylcitalopram (*S*-**3**) in wt hSERT, Tyr95Phe, and Asp98Glu mutant constructs. For wt hSERT, the inhibitory potency decreases according to the number of methyls removed, from 9.2 nM (*S*-**1**) to 48 nM (*S*-**2**) and 520 nM (*S*-**3**) (Table 2). This supports the idea that the methyl groups are important in bridging between Asp98 and Tyr95, and is further supported by the polarized *N*-methyl groups as reflected in the QPLD calculations. Consequently, the bridging allows for a stabilizing delocalization of the positive charge toward both Asp98 and Tyr95 in wt hSERT. In the Tyr95Phe mutant, the loss of affinity is not seen until both methyls are removed: 132 nM (*S*-**1**) to 61 nM (*S*-**2**) to 860 nM (*S*-**3**). This overall loss of affinity and the lack of specificity of the Tyr95Phe mutant (K_i = 132 nM (*S*-**1**), K_i = 61 nM (*S*-**2**), p = 0.63) toward the second methyl compared to wt hSERT (K_i = 9.2 nM (*S*-**1**), K_i= 48 nM (*S*-**2**), p = 0.0079) supports the idea that a methyl group interacts favorably with the hydroxyl group of Tyr95 (Figure 3).

The length of the side chain of Asp98 has previously been shown to affect inhibitory potency of racemic citalopram.[34,41] Likewise, the Asp98Glu mutation dramatically affects inhibitory potency for *S*-**1**; an increase from 9.2 nM (wt) to 560 nM (Asp98Glu), which represents a 61-fold decrease in affinity (p < 0.00005), was found. The removal of one methyl (*S*-**1** to *S*-**2**) resulted in a 5-fold loss of affinity for wt hSERT; however, the same loss of affinity is not seen for the less methylated forms of the ligands in the Asp98Glu mutant. On the contrary, a gain of affinity is noted when both methyls are removed: 560 nM (*S*-**1**) to 770 nM (*S*-**2**) to 170 nM (*S*-**3**). Two opposing tendencies may be relevant here; first, the Asp98Glu mutation may remove the acidic group partially from its usual environment and possible binding partners. This would manifest itself in an altered rank-order potency exhibited by the demethylated ligands of *S*-**1** if these methyls engage in delocalization of the charge to neighboring residues, and second, the added bulk of Asp98Glu may introduce steric issues that favor a less methylated analogue. Again, the mutation disrupts the normal bridging of Asp98 and Tyr95 by the dimethylammonium ion, which can be observed by *S*-**1** becoming less potent and removing the gain of affinity normally associated with the second methyl group. At the same

(56) Scrutton, N. S.; Raine, A. R. C. *Biochem. J.* **1996**, *319*, 1–8.

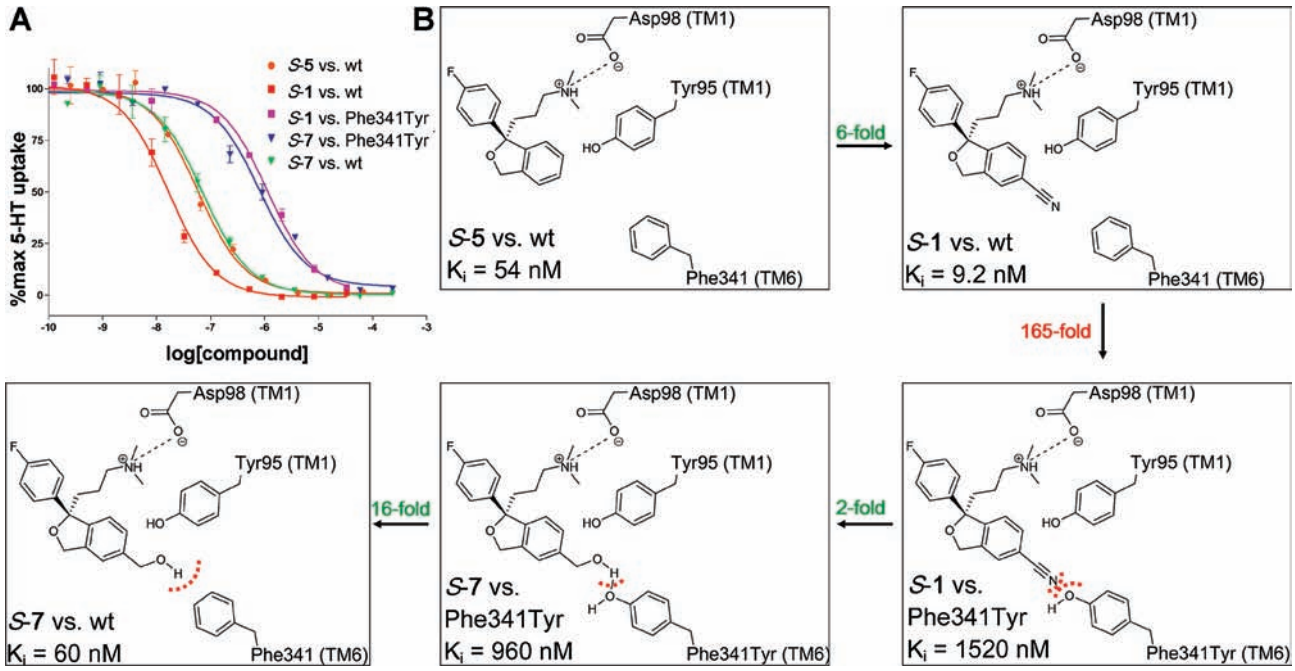

Figure 4. (A) 5-HT uptake curves revealing the interaction of Phe341 with the cyano group of *S*-citalopram. (B) PaMLAC scheme showing the relationship between the cyano group of *S*-**1** and Phe341 in hSERT. Fold changes in red specify loss of affinity, whereas green numbers indicate gained affinity.

time the fact that *S*-**3** is 5-fold more potent than *S*-**2** (770 to 170 nM, $p < 0.00005$) indicates that the added volume of the Asp98Glu mutation introduces steric strain that may be alleviated by simultaneous removal of volume from the ligand in terms of demethylation.

The above observations are in full accordance not only with the results from the docking of *S*-citalopram, but also with previous indications of ionic interactions between ligands and Asp98[15,41] and records of Tyr95 as an important residue in antidepressant binding.[34,36]

***S*-Citalopram - Fluorine Atom.** The ***S*-ClusterII** has the fluorophenyl group embedded in a pocket lined by Ala173, Asn177, and Thr439 (Figure 1 B). Possible polar interactions between the electronegative fluorine atom and residues at the bottom of this hydrophilic pocket can be envisioned with distances of approximately 3.4−3.7 Å to the side chain amide of Asn177 and the hydroxyl group of Thr439. The *in silico* predicted housing of the *S*-**1** fluorine atom in this pocket was examined by determining the inhibitory potencies of *S*-citalopram and its analogue, *S*-(CH_2OH, CN) (*S*-**4**), in wt hSERT, and seven mutants of Ala173, Asn177, and Thr439.

The inhibitory potency of *S*-citalopram is not affected by any of the mutations in the hydrophilic pocket (Table 3), but changing the fluorine atom to a CH_2OH group in *S*-**4** causes a 9-fold loss of affinity in wt hSERT (9.2 nM (*S*-**1**), 83 nM (*S*-**4**), $p < 0.00005$). As for *S*-**1**, the inhibitory potency of *S*-**4** is not affected by the Ala173Ser, Thr439Ala, or the Thr439Ser mutations. Conversely, the Ala173Met mutation causes a 48-fold reduction of inhibitory potency of *S*-**4** (4000 nM) compared to wt hSERT (83 nM). Either a steric conflict between the methionine and the CH_2OH group or repulsion between the hydrophobic methionine and the hydrophilic CH_2OH accounts for the observed loss in inhibitory potency. When Asn177 is mutated to shorter side-chain residues (alanine, serine, and threonine), 5−14 fold losses of affinity when substituting the fluorine atom to CH_2OH group (*S*-**4**) are measured. The penalty correlates with the hydrophobicity of the side chain (alanine 14-fold, threonine 10-fold, serine 5-fold) in accordance with the results from the Ala173Met mutant. This dependence on hydrophobicity supports the placement of the hydrophilic CH_2OH group in a hydrophilic pocket lined by Ala173 and Asn177. Combined, the data underpins the computationally predicted position of the fluorine atom of ***S*-ClusterII** in the hydrophilic pocket, which we have earlier found to also harbor the 5-hydroxy moiety of 5-HT.[15]

***S*-Citalopram - Cyano Group.** In ***S*-ClusterII** the cyano group is pointing toward the extracellular vestibule with the nitrogen atom being in the vicinity of Phe335 and Phe341 (Figure 1 B). Therefore, the inhibitory potency of *S*-citalopram and cyano replaced analogues, *S*-(F,H), *S*-(F,$COOCH_3$), and *S*-(F, CH_2OH), *S*-**5**, *S*-**6**, and *S*-**7**, respectively, were determined in wt hSERT as well as Phe335Asn, Phe335Tyr, and Phe341Tyr mutants. Either removal of the cyano group (*S*-**5**, 54 nM) or a CH_2OH substitution (*S*-**7**, 60 nM) causes a 6-fold decrease in inhibitory potency in wt hSERT compared to that of *S*-citalopram (9.2 nM). Furthermore, substituting the cyano group with the sterically more demanding $COOCH_2CH_3$ group in *S*-**6** (86 nM) yields a 9-fold decrease in affinity.

The Phe335Asn and Phe335Tyr mutations do not have any significant effect on either the inhibitory potencies of *S*-citalopram or on those of the *S*-**5**, *S*-**6**, and *S*-**7** analogues. The Phe341Tyr mutant (1520 nM), however, exhibits a staggering 165-fold loss of affinity for *S*-citalopram compared to wt hSERT (9.2 nM). The remarkable magnitude in loss of affinity for *S*-citalopram in the Phe341Tyr mutant is not observed to the same extent for *S*-**5** (35-fold), *S*-**6** (28-fold), or *S*-**7** (16-fold) in this mutant. The full PaMLAC scheme for this relationship between the cyano group of *S*-**1** and Phe341 in hSERT is outlined in Figure 4 along with measured uptake inhibition curves. Starting with the unsubstituted *S*-**5**, the introduction of the cyano group in *S*-**1** is beneficial to affinity (6-fold), but when simultaneously introducing the Phe341Tyr mutation a sterical clash or partial charge repulsion between the cyano group of *S*-**1** and the hydroxyl group of the Phe341Tyr protein results in

a dramatic 165-fold loss of affinity. This loss of affinity is partially (2-fold) reversed by changing the cyano group to the more flexible hydroxymethyl as in *S*-**7** and fully reversed (16-fold increase) by removing the obstructing hydroxyl group from residue 341. These observations strongly support the modeling result, where the cyano group of ***S*-ClusterII** is found in the vicinity of the 4-position of Phe341.

***R*-Citalopram - Ammonium Ion.** The modeling calculations predicted the dimethylammonium ion to be situated in the electron-rich pocket lined by Tyr95 and Asp98. Therefore, the Tyr95Phe and the Asp98Glu mutants were again used to investigate the anchoring of the positively charged ammonium ion of the ligand to the protein. As for *S*-**1**, the inhibitory potency of *R*-**1** decreases in the Tyr95Phe and Asp98Glu constructs compared to wt hSERT with K_i values of 370 nM (wt), 820 nM (Tyr95Phe), and 1740 nM (Asp98Glu), respectively. This indicates that the ammonium ion of *R*-**1** is similarly located between these two residues. Contrary to what was found for *S*-**2**, the *R*-**2** analogue does not significantly change the effect of the Asp98Glu mutation; rather, *R*-**2** (37 nM) showed increased inhibitory potency compared to *R*-**1** in wt (370 nM).

***R*-Citalopram - Fluorine Atom.** In ***R*-ClusterI** the fluorine atom is pointing toward the extracellular vestibule; this is similar to what was seen for the cyano group in ***S*-ClusterII** (Figure 1 B). The inhibitory potencies of *R*-**1** and *R*-**4**, *R*-(CH_2OH,CN), were determined in wt hSERT and the Phe335Asn, Phe335Tyr, and Phe341Tyr mutant constructs. The Phe335Asn mutant had no impact on the inhibitory potency of the two ligands. The Phe335Tyr mutant showed 4-fold higher affinity for *R*-**1** (370 nM (wt), 86 nM (Phe335Tyr), $p = 0.0005$) and 3-fold higher affinity for *R*-**4** (1050 nM (wt) 390 nM (Phe335Tyr), $p = 0.0056$), compared to wt hSERT. Furthermore, the Phe341Tyr mutant induced 6-fold decreases in inhibitory potency of *R*-**1**; K_i values of 370 nM (wt) and 2200 nM (Phe341Tyr), respectively, whereas K_i values for *R*-**4** of 1050 nM (wt) and 5800 nM (Phe341Tyr) were observed.

The fluorophenyl group in ***R*-ClusterI** is not only in proximity to Phe335 and Phe341 but also close to Tyr175, Tyr176 and Thr497. Thus, the compounds *R*-**1** and *R*-**4** were also tested for inhibitory potencies in the Tyr175Phe and the Tyr176Phe constructs. In addition, constructs where Thr497 was mutated to alanine, valine, leucine, or serine were tested. Tyr176Phe showed decreased inhibitory potencies of approximately 3-fold for all *R*-compounds, whereas Tyr175Phe showed increased inhibitory potencies of approximately 4-fold for all *R*-compounds (Table 3). None of the mutations at position 497 had significant effect on the inhibitory potencies of *R*-compounds; hence, the SAR data do not allow us to reach definitive conclusions about the location of the *R*-**1** fluorine atom.

***R*-Citalopram - Cyano Group.** The ***R*-ClusterI** of *R*-citalopram has the cyano group embedded in the hydrophilic pocket lined by Ile172, Ala173, Asn177, and Thr439 (Figure 1 C). Again, the Ala173Ser, Ala173Met, Asn177Ser, Asn177Ser, Asn177Thr, Thr439Ala, and Thr439Ser mutant constructs together with the wt hSERT were examined for binding of *R*-**1** and the cyano-deprived (*R*-**5**) or cyano-substituted analogues (*R*-**6** and *R*-**7**). The mutations at position 173 and 439 had only minor effect on the inhibitory potency of *R*-**1** (Table 3). The same ratios of K_i values as those for *R*-**1** between wt and Ala173 and Thr439 mutants were observed for *R*-**6** and *R*-**7** (Table 3). This indicates no significant effect from these ligands. The inhibitory potency of *R*-**5**, however, increased 10-fold in the Ala173Met mutant, with K_i values of 730 nM (wt) and 73 nM (Ala173Met). Compared to the 2-fold increase in affinity observed for *R*-**1** in the same mutant, the data support that the cyano group fills a void in the binding pocket close to Ala173. Consequently, when this pocket is unoccupied by the cyano group, it is possible to complement the missing hydrophilic substituent by filling this pocket with a longer hydrophobic side chain at position 173 (Ala173Met), thereby, regaining the inhibitory effect of *R*-**5**.

We also shortened the side chain of Asn177 by mutation to alanine, serine, or threonine. This maneuver provided a relative gain of function for the cyano-deprived *R*-**5** (by 2−4 fold) and the COOEt-substituted analogue, *R*-**6** (by 5−7 fold), whereas a substitution of the cyano group to a hydroxymethyl (*R*-**7**) did not show significant gain of function. The data implies that the removal of the Asn177 side chain renders the pocket more hydrophobic, thereby favoring analogues of *R*-citalopram with hydrophobic substituents at the 5-position of the dihydroisobenzofuran ring or, alternatively, the analogue, *R*-**5**, where the hydrophilic cyano group is removed.

The compiled observations support the prediction of the cyano group of *R*-**1** to be located in the hydrophilic pocket lined by Ala173, Asn177, and Thr439 as in ***R*-ClusterI**.

Discussion

The molecular modeling study of *S*- and *R*-citalopram to the substrate binding site in the refined hSERT homology model resulted in the vast majority of the poses for both enantiomers being located inside the central cavity and not in the extracellular vestibule. This is similar to what has been found for TCA binding to hSERT[27] and for cocaine binding to hDAT[13] but contrary to the weak noncompetitive binding site for TCAs and some SSRIs in the vestibular site of LeuT,[17−19] speculated to be relevant for hSERT.[17,18] *R*- and *S*-citalopram could be docked into the vestibule site with the fluorine atom placed in the proposed halogen binding pocket. With 5-HT in the central binding cavity, mimicking the published LeuT structures with antidepressants in the vestibular site and a leucine molecule in the central cavity, the computed scores were −7.5 kcal/mol for *S*-**1**, which is significantly less favorable for the high-affinity enantiomer than when docked into the primary site, and around −9.2 kcal/mol for *R*-**1**. If the elusive allosteric site[57] was located in the putative hSERT S2-site, it would be consistent with our docking studies and also provide a simple mechanism for the allosteric effect on antidepressant dissociation from the central primary site. However, it would be at odds with detailed studies employing cross-species chimeras and binding kinetics[58,59]

Two possible orientations for each enantiomer were identified for binding to the substrate binding pocket. Various computational methods and techniques were utilized to differentiate between these. Clear indications were found that the most likely binding mode of *S*-citalopram inside the central binding site places the fluorophenyl group close to the hydrophilic pocket lined by Ala173, Asn177, and Thr439, and the cyano group pointing toward the volume lined by Phe335 and Phe341. The most likely binding mode of *R*-citalopram was slightly more difficult to predict solely from the computational methods, though a trend toward ***R*-ClusterI** was established. Computational and experimental results show that the two enantiomers

(57) Plenge, P.; Mellerup, E. T. *Eur. J. Pharmacol.* **1985**, *119*, 1–8.
(58) Neubauer, H. A.; Hansen, C. G.; Wiborg, O. *Mol. Pharmacol.* **2006**, *69*, 1242–1250.
(59) Zhong, H.; Hansen, K. B.; Boyle, N. J.; Han, K.; Muske, G.; Huang, X.; Egebjerg, J.; Sánchez, C. *Neurosci. Lett.* **2009**, *462*, 207–212.

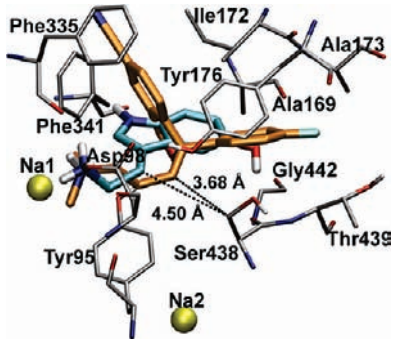

Figure 5. Overlay of 5-HT[15] (cyan) and *S*-citalopram (orange) from ***S*-ClusterII** with the distances between the carbon attached to the aromatic group of the two alkyl amine arms and Cβ of Ser438 shown. Important residues of hSERT with bound *S*-citalopram are shown in gray.

share a common position of the ammonium ion in the pocket between Tyr95 and Asp98 (Figure 3). Similarly, Asp98 coordinates the substrate 5-HT via a stabilizing salt bridge between the acidic moiety of this residue and the positively charged ammonium ion of the substrate.[15,53] *S*-**1** affinity is highly sensitive to Tyr95Phe and Asp98Glu mutations; these eliminate the loss of affinity normally associated with demethylation of the ligand and demonstrate that the interaction network between Asp98 and Tyr95 mediated by the charged ammonium ion is disrupted by either mutation. Thus, the disruption normally associated with removal of a methyl when bound to wt hSERT no longer plays a role in either mutant because this disruption is already brought about by the mutation. It illustrates that successful bridging of Asp98 and Tyr95 by the ligand is very important for the high affinity of at least *S*-citalopram, and likely also for other antidepressants with a tertiary ammonium ion.

The location of the fluorine atom and cyano group of the two enantiomers firmly defines the orientation of the ligand within the binding site when taken together with the overlapping location of the amine. Our data shows that they are oriented inversely to each other with regard to the two aromatic moieties (Figure 1). The pocket between Ala173 and Thr439 was previously shown to accommodate the 5-hydroxy group of 5-HT.[15] In this study we show that this same pocket accommodates the fluorine atom of *S*-**1** (Figure 5), whereas it is occupied by the cyano group of *R*-**1**. Similarly, *S*- and *R*-citalopram have different functional groups located in the area between Phe335, Phe341, and Thr497.

Two other accounts have appeared suggesting binding modes of *S*-citalopram in hSERT.[12,16] However, neither of these studies included the chloride ion in the models. The chloride ion is located less than 7 Å from the binding site; thus, it may affect the electrostatic nature of this cavity, though a recent study shows that the effect of the chloride ion is not sufficient to differentiate between different ligands.[60] In both previous studies, the dimethylammonium ion is found close to Asp98 similar to our studies. The fluorophenyl and the cyano groups of *S*-**1** are, however, reversed in our model compared to Jørgensen et al.[12] who used manual docking and manual reorientation of the protein side chains to accommodate *S*-**1** in the binding site. Consequently, that study only deals with a single orientation of *S*-**1** and would therefore not explore an orientation as found in ***S*-ClusterII**. The conclusion reached in the second study[16] has the methyl group of the ammonium ion in close proximity of Ser438, with a distance between the nitrogen atom and Ser438(Cβ) of approximately 4 Å, placing the nitrogen atom in the other favorable area of the MIFs in Figure 2 E. That study is based on changes in binding affinity upon mutation of Ser438 and subsequent complementation by racemic citalopram analogues with varying degrees of methylation. Partial rescue of the affinity lost by removing a methyl group on the ligands was seen by adding a methyl to the protein in a Ser438Thr mutant. However, shortening of the dimethylaminopropyl chain by one carbon also almost completely rescues the affinity.[16] In our preferred models, the distance from the ammonium ion to Ser438(Cβ) is slightly longer (6−7 Å), which indicates that there is no direct interaction between the two groups. A similar situation has been suggested for imipramine binding to hSERT.[16,27] In ***S*-ClusterII** a Ser438Thr mutation would indeed place the added methyl at position 438 inside the binding pocket and consequently push the ligand further toward Asp98 (Figure 5). The observed recovery of affinity can thus be rationalized by the favorable shortening of the alkyl amine chain when the binding site has to accommodate an extra methyl group in the protein.

Why Is an Inhibitor like *S*-Citalopram Not Transported? The most striking result from the SAR-data is the enormous loss of affinity for *S*-**1** in the Phe341Tyr mutant construct. The minute change of adding a hydroxyl group to this residue changes the K_m value of 5-HT only 3-fold and causes no significant difference in V_{max} for 5-HT (data not shown). In this context the staggering 165-fold decrease in inhibitory potency of *S*-**1** strongly indicates that this residue is a key determinant of the high-affinity inhibition by *S*-citalopram. Other mutations than tyrosine (serine, cysteine, and tryptophan) at position 341 were not well tolerated, with respect to keeping a functional transporter, supporting the vital function played by the phenyl group of this residue.[15,61] Phe341 is situated in the unwound part of TM6 which, along with the similar part of TM1 of the otherwise rigid α-helical folded core of the protein, is suggested to provide the flexibility needed to allow for the large conformational change during transport of substrate.[11,62] The flexible backbone amide of Phe341 forms a hydrogen bond with Glu136 (Figure 6 A), which is also involved in an interaction with Glu508 in TM10 of hSERT (Figure 6 B), corresponding to Glu62 and Glu419 in LeuT.[38] Glu136 has been found to be important for a conformational switch during the transport cycle,[63] which was speculated to be governed by the hydrogen-bonding potential of its side chain; when the hydrogen-bonding potential is destroyed, the transporter adopts an inward-facing conformation.[63] As a consequence of this, a possible explanation could be that this native hydrogen bond between Glu136 and the backbone of Phe341 may be broken to facilitate transport of the substrate. Conversely, a ligand-induced stabilization of this hydrogen bond could potentially prevent translocation. Furthermore, the unwound part of TM6 is in contact with Ala505 in TM10 with a distance between the methyl group of Ala505 and Gly340(Cα) measuring around 4.1 Å in our models. The change of Ala505 to the larger valine is known to improve

(60) Tavoulari, S.; Forrest, L. R.; Rudnick, G. *J. Neurosci.* **2009**, *29*, 9635–9643.
(61) Celik, L.; Schiøtt, B.; Tajkhorshid, E. *Biophys. J.* **2008**, *94*, 1600–1612.
(62) Forrest, L. R.; Zhang, Y.; Jacobs, M. T.; Gesmonde, J.; Xie, L.; Honig, B. H.; Rudnick, G. *Proc. Natl. Acad. Sci. U.S.A.* **2008**, *105*, 10338–10343.
(63) Korkhov, V. M.; Holy, M.; Freissmuth, M.; Sitte, H. H. *J. Biol. Chem.* **2006**, *281*, 13439–13448.

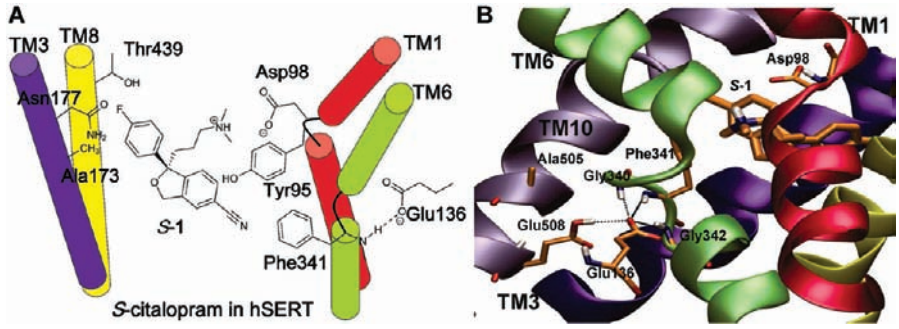

Figure 6. (A) Schematic placement of *S*-**1** in the central binding site of hSERT, highlighting the observed interactions. (B) Hydrogen bonding network between the unwound part of TM6 and residues from TM3 and TM10.

the affinity of another high-affinity inhibitor, imipramine,[64] as well as reduce the self-potentiating allosteric effect of *S*-citalopram,[58] indicating that affecting the interaction network of the flexible part of TM6 by increasing the bulk of an adjoining helix (TM10) might effect ligand binding and perception. Combined, these observations could suggest that, not only is the flexible region in TM6 a necessary structural requirement to allow other parts of the protein to move, it may also be subject to tight regulation with regards to discriminating between substrates and inhibitors. Stabilization of the hydrogen bond between the backbone amide of Phe341 and Glu136 could be pivotal for obtaining inhibition of hSERT.

Conclusions

To summarize, we provide strong support for reversed binding modes of the high-affinity SSRI *S*-citalopram (***S*-ClusterII**) and its low-affinity *R*-enantiomer (***R*-ClusterI**). Our findings emphasize the importance of providing homochiral drugs. Several computational methods together with experimental data on inhibitory potencies of optically pure citalopram analogues for wt hSERT and mutants have made it possible to reveal the difference in binding of *S*- and *R*-citalopram. Furthermore, we identify the citalopram binding site to be overlapping with the substrate binding site. This binding site is clearly different from the promiscuous low-affinity, noncompetitive binding site found in LeuT.[18,20] Contrary to the vestibular site in LeuT, the central binding site for citalopram identified herein readily accounts for the high-affinity, sodium-dependent, competitive binding of SSRIs to their relevant pharmaceutical human target, hSERT. Finally, this study has made it possible to suggest key structural elements that provide the basis for the high-affinity binding of *S*-citalopram. The same structural elements may be exploited in future pharmacological research.

Acknowledgment. The research was supported by grants from the Lundbeck, Carlsberg and Novo Nordisk Foundations, the Danish Natural Science Research Council and the Danish National Research Foundation. Computations were possible through allocations of time at the Centre for Scientific Computing, Aarhus. We thank H. Lundbeck A/S for generous supply of *S*- and *R*-citalopram and other analogues, and Dr. Robert Dancer (H. Lundbeck A/S) for useful discussions and practical assistance, as well as Aarhus Graduate School of Science (AGSoS), iNANOSchool and OChem School for financial support.

Supporting Information Available: Details of the computational and experimental methods are included as well as tables (with GlideScore, IFDScore, bond distances for Asp98•••N^+, partial charges from QPLD, docking in the S2-site, and physical data for chiral analogues) and NMR spectra of synthesized compounds. This material is available free of charge via the Internet at http://pubs.acs.org.

JA906923J

(64) Severinsen, K.; Sinning, S.; Muller, H. K.; Wiborg, O. *J. Neurochem.* **2008**, *105*, 1794–1805.